Electronic Supplementary Material (ESI) for Journal of Materials Chemistry B.

Supporting Information

Unraveling the Molecular Mechanisms of Thermo-responsive Properties of Silk-Elastin-Like Proteins by Integrating Multiscale Modeling and Experiment

Jingjie Yeo Wenwen Huang, Anna Tarakanova Yong-Wei Zhang, David L. Kaplan and Markus J. Buehler*

*mbuehler@MIT.EDU

CHARMM Potential and Implicit Solvent

The CHARMM potential energy function[1] is given by:

$$U_{CHARMM} = \sum_{bonds} K_{bond}(b_{ij} - b_0)^2 + \sum_{angles} K_{ang}(\theta_{ijk} - \theta_0)^2 + \sum_{dihedrals} K_{dih}[1 + \cos(n\phi_{ijkl} - \delta)] + \\ + \sum_{improper} K_{imp}(w_{ijkl} - w_0)^2 + \sum_{nonbonded} \left\{ \varepsilon_{ij} \left[\left(\frac{\sigma_{ij}}{r_{ij}} \right)^{12} - 2 \left(\frac{\sigma_{ij}}{r_{ij}} \right)^{6} \right] + \frac{q_i q_j}{4\pi D r_{ij}} \right\}$$

where K_{bond}, K_{ang}, K_{dih}, $K_{1,3}$, and K_{imp} are the bond, angle, dihedral angle, Urey–Bradley, and improper dihedral angle force constants, respectively; b_{ij}, θ_{ijk}, φ_{ijkl}, S_{ik}, and ω_{ijkl} are the bond length, bond angle, dihedral angle, Urey–Bradley 1,3-distance, and improper torsion angle, respectively; zero-subscripted terms are the equilibrium values for the respective terms; n is the periodicity and δ the phase of a torsion; ε_{ij} is the well depth of the Lennard-Jones (LJ) potential; σ_{ij} is the distance at the LJ minimum; q is the partial atomic charge; D is the effective dielectric constant; and r_{ij} is the distance between any atoms i and j.

In implicit solvent simulations, the CHARMM potential energy function above is modified with a solvation energy term, such that the effective energy of the solvated protein becomes

$$U_{eff} = U_{intra} + \Delta G^{solv}$$

where U_{intra} is the intramolecular energy and ΔG^{solv} is solvation free energy.

PLUM Coarse-grain Potential

The PLUM potential[2] is a coarse-grained peptide model of intermediate resolution with implicit water solvent. The coarse-graining scheme is depicted in **Figure S1** with alanine tripeptides as an example. All amino acids are coarse-grained into beads representing the N- and C-terminus, the α-carbon, and the entire sidechain (N, C, C_α, and C_β, respectively). The exception is glycine which lacks a sidechain bead. The potential energy function to describe the bonded interactions are given by

$$U_{PLUM,\,bonded} = \sum_{bonds} K_{bond}(b_{ij} - b_0)^2 + \sum_{angles} K_{ang}(\theta_{ijk} - \theta_0)^2 + \sum_{dihedrals} K_{dih}[1 - \cos(n\phi_{ijkl} - \delta)]$$

Nonbonded interactions are split into multiple potential energy terms.

Backbone beads interact as

$$U_{bb} = \begin{cases} 4\varepsilon_{bb}\left[\left(\frac{\sigma_{ij}}{r_{ij}}\right)^{12} - \left(\frac{\sigma_{ij}}{r_{ij}}\right)^{6} + \frac{1}{4}\right], & r \le r_C \\ 0, & r > r_c \end{cases}$$

Sidechain interactions vary according to their hydrophobicity and the potential energy function is expressed as

$$U_{hp} = \begin{cases} 4\varepsilon_{hp}\left[\left(\frac{\sigma_{C_\beta}}{r_{ij}}\right)^{12} - \left(\frac{\sigma_{C_\beta}}{r_{ij}}\right)^{6} + \frac{1}{4}\right] - \varepsilon_{hp}\varepsilon_{ij}^{'}, & r \le r_C \\ 4\varepsilon_{hp}\varepsilon_{ij}^{'}\left[\left(\frac{\sigma_{C_\beta}}{r_{ij}}\right)^{12} - \left(\frac{\sigma_{C_\beta}}{r_{ij}}\right)^{6}\right], & r_C \le r \le r_{HP,cut} \\ 0, & r > r_{HP,cut} \end{cases}$$

Hydrogen bonding and dipole interactions are modelled explicitly to account for the lack of hydrogen atoms and partial charges in the CG beads. The hydrogen bonding potential is a combination of a radial 12-10 Lennard-Jones potential and an angular term

$$U_{hb} = \varepsilon_{hb}\left[5\left(\frac{\sigma_{hb}}{r_{ij}}\right)^{12} - 6\left(\frac{\sigma_{hb}}{r_{ij}}\right)^{10}\right] \times \begin{cases} \cos^2\theta_N \cos^2\theta_C, & |\theta_N|, |\theta_C| < 90° \\ 0, & otherwise \end{cases}$$

The dipole interactions are expressed as

$$U_{dip} = k_{dip}[(1 - \cos\phi) + (1 - \cos\psi)]$$

Replica Exchange MD

REMD improves protein conformational sampling through the application of Monte Carlo exchanges into classical MD simulation schemes[3]. Systems with identical initial configurations are replicated and the initial velocities of each replica are applied according to a pre-determined range of temperatures. High temperatures prevent the protein from being trapped in local energy minima, thereby broadly sample conformational space. Frequent exchanges between replicas ensure that energetically favorable configurations are propagated to lower temperatures. Exchanges between two replicas *i* and *j* are accepted based on the probability, *P,* given by the Metropolis criterion

$$P = \begin{cases} 1, & \Delta \le 0 \\ \exp(-\Delta), & \Delta > 0 \end{cases}$$

where

$$\Delta = (\beta_i - \beta_j) \cdot (E_i - E_j)$$

and

$$\beta = \frac{1}{k_b T}$$

Supplementary Figures

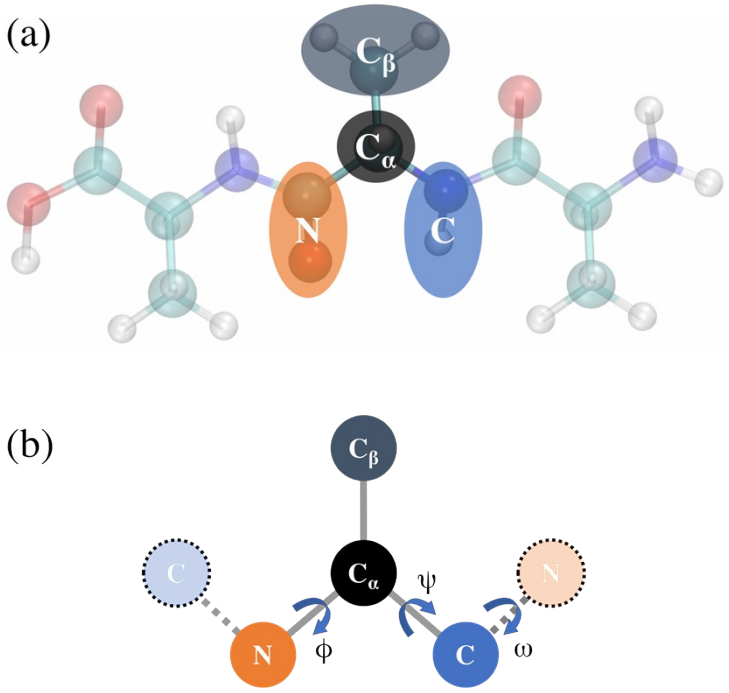

Figure S1. (a) Coarse-graining scheme for the PLUM potential. (b) Illustration of the local geometry in each CG amino acid.

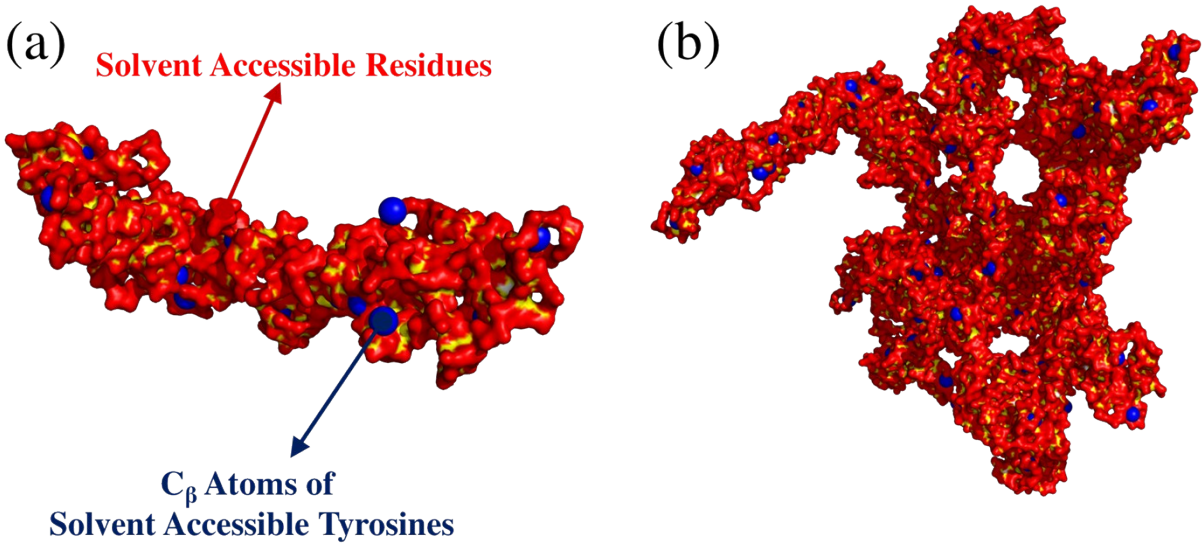

Figure S2. (a) To crosslink SE_{8Y} molecules, C_β atoms of solvent accessible tyrosines (blue beads) were identified by determining the solvent accessible surface of the molecule (red surface). (b) Final morphology of ten crosslinked SE_{8Y} molecules.

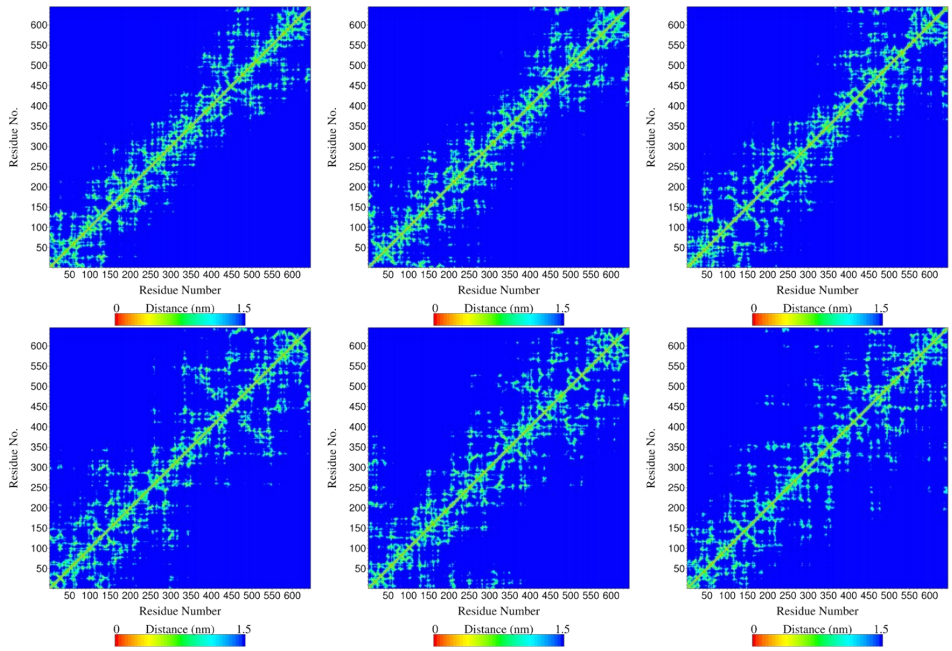

Figure S3. From left to right and top to bottom, contacts maps of a single SE_{8Y} molecule in the temperature range of 277K, 287K, 297K, 307K, 317K, and 330K respectively. These figures show the molecule's structural transition manifest as greatly increased numbers of contacts between any residues *i* and residues that are further than *i*±*3*.

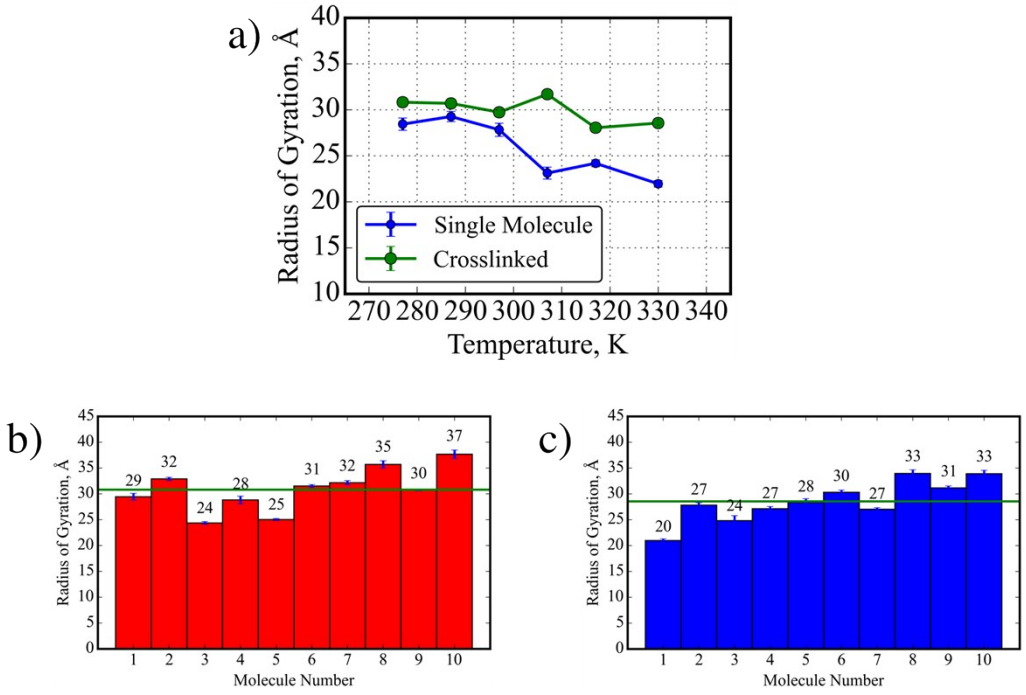

Figure S4. (a) Detailed comparison of the variation in radius of gyration of a single SE_{8Y} molecule versus a cluster of ten crosslinked SE_{8Y} molecules, where the crosslinked cluster had drastically diminished temperature response. (b), (c) Change in the radius of gyration for every molecule in the crosslinked cluster at the temperatures of (b) 277 K and (c) 330 K.

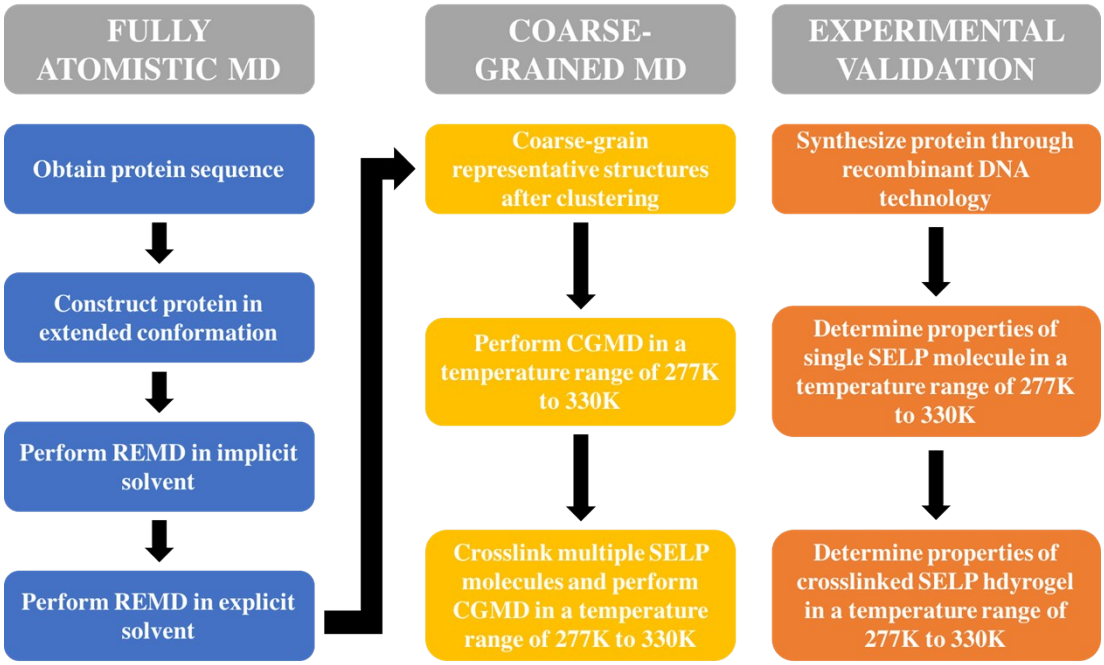

Figure S5. Schematics of the modelling, simulation, and experimental process to cross-validate all data obtained, thus providing comprehensive understanding of both macroscale and molecular phenomena associated with the concentration dependent deswelling of SELP hydrogels.

Supplementary References

1. B. R. Brooks, R. E. Bruccoleri, B. D. Olafson, D. J. States, S. Swaminathan and M. Karplus, *J Comput Chem*, 1983, **4**, 187-217.
2. T. Bereau and M. Deserno, *The Journal of Chemical Physics*, 2009, **130**, 235106.
3. Y. Sugita and Y. Okamoto, *Chem Phys Lett*, 1999, **314**, 141-151.